New Generalized Newtonian Fluid Models for Quantitative Description of Complex Viscous Behavior in Shear Flows

Ryszard Steller,[1] Jacek Iwko [2]
[1]*Polymer Engineering and Technology Department, Faculty of Chemistry, Wrocław University of Science and Technology, Wybrzeże Wyspiańskiego 27, Wrocław 50-370, Poland*
[2]*Faculty of Mechanical Engineering, Chair of Foundry, Plastics and Automation, Wrocław University of Science and Technology, Wybrzeże Wyspiańskiego 27, Wrocław 50-370, Poland*

Two semiempirical models of generalized Newtonian fluid are discussed. Special attention was focused on the stress dependent model based on the free volume theory. However, the strain-rate dependent model in form of a modified viscosity function resulting from Oldroyd equation is also presented. Both models (along with specific cases) reflecting pseudoplastic or dilatant behavior of liquids in shear flows are generalized to multimode models (defined as products of two or more basic models), which are able to describe quantitatively the behavior of more complex systems, for example, systems with pseudoplastic and dilatant properties in different shear stress (shear rate) ranges. A number of practical examples for viscosity curves of non-Newtonian fluids described by these models are given. The questions of inverse models and model efficiency are also discussed. POLYM. ENG. SCI., 00:000–000, 2017.

INTRODUCTION

Various models of the generalized Newtonian fluid, that is, the Newtonian fluid with strain-rate or stress dependent viscosity, are widely applied for description of flows, in which the viscous effects dominate. The most frequent cases of such flows are the steady shear flows in processing machines, pipelines, measuring devices, etc. These models can also be useful for the analysis of structure changes of various liquids in dependence on flow conditions.

The constitutive equation of generalized Newtonian fluid (GNF) can be formulated in the following way, for example, Ref. 1:

$$T=2\eta(II_T)D \tag{1}$$

or

$$T=2\eta(II_D)D \tag{2}$$

where the viscosity η is a function of the second invariant of the rate-of-strain tensor D or the extra-stress tensor T.

So far, many empirical, semiempirical, and theoretical equations for description of viscosity as a function of stress or much more frequently of strain-rate have been proposed. Probably, the most comprehensive array of about 30 viscosity equations and a similar number of specific equations for suspensions was presented by Yilmaz and Gundogdu [2] in the work devoted to the problems of blood rheology. More meager arrays are included in almost every book or monograph from different domains of rheology comprising polymers [3], foods [4], cosmetics and toiletries [5], slurries [6], and many other. These equations pertain to viscous or viscoplastic liquids without taking into account many formulas resulting from theories of viscoelastic polymer liquids, for example, Refs. 7 and 8. However, the generalized Newtonian models are frequently applied when analyzing the steady shear flows of viscoelastic liquids. Some more detailed problems connected with GNF models will be considered later.

The goal of this work is the discussion and assessment of two novel semiempirical equations (with several specific cases) for quantitative description of shear viscosity curves of different non-Newtonian fluids.

The first one based on the free volume theory makes the viscosity dependent on the stress level according to the expression (*Eq. 1*) and has the form of the following four-parameter model:

$$\eta=\eta_0\exp\left(-\frac{\delta\tau^n}{1+\alpha\tau^n}\right) \tag{3}$$

where η_0, n, α, δ are material constants and the stress $\tau=\sqrt{0.5II_T}$ is determined by the second invariant of the extra-stress tensor T.

The second equation represents the viscosity as a function of the strain-rate according to the expression (*Eq. 2*). It can be formally treated as the empirical generalization of the viscosity function resulting from some constitutive equations of viscoelastic liquids, for example, from the Oldroyd equation (8). It has the form of the five-parameter model:

$$\eta=\eta_o\left[\frac{1+(\lambda_1\dot\gamma)^v}{1+(\lambda_2\dot\gamma)^v}\right]^\mu \tag{4}$$

where η_0, λ_1, λ_2, μ, v are material constants and the strain-rate $\dot\gamma=\sqrt{0.5II_D}$ is determined by the second invariant of the rate-of-strain tensor D.

For description of more complicated viscosity curves, for example, with pseudoplastic and dilatant regions in different shear stress/shear rate ranges, the presented equations can be generalized to multimode models expressed formally as products of two or more basic equations from one of the main groups. The questions of inverse models and the model efficiency (adequate data description by models with minimal number of parameters) are also discussed.

STRESS-DEPENDENT VISCOSITY MODELS

It was already mentioned that the stress dependent GNF model discussed in this paper in form of the equation (*Eq. 3*) is

Correspondence to: J. Iwko; e-mail: jacek.iwko@pwr.edu.pl
DOI 10.1002/pen.24741
Published online in Wiley Online Library (wileyonlinelibrary.com).

based on the free volume theory, which was also successfully applied for description and interpretation of many other phenomena observed in different systems, for example, glass transition, diffusion, plasticization, viscosity dependence on temperature and pressure, viscosity of multicomponent systems, etc. The free volume theory assumes that the viscosity η as a measure of internal friction during flow becomes lower if the content of space unfilled with molecules, that is, the free volume V_{fr}, increases in respect to the true volume of molecules, that is, the occupied volume V_{oc}. The sum of both volumes creates the macroscopic specific volume V of a material. The mathematical expression for the free volume theory is the Doolittle equation (9), which can be written as:

$$\eta = K \cdot \exp\left(B \frac{V_{oc}}{V_{fr}}\right) \tag{5}$$

where B and K are material constants.

Hereafter, the following abbreviation will be used:

$$\theta = B \frac{V_{oc}}{V_{fr}} \tag{6}$$

The free volume V_{fr} is generally determined by the mobility of molecules. For this reason it may undergo significant changes under the action of temperature, pressure, internal stresses, etc., in contrast to the occupied volume V_{oc}, which remains almost constant. For instance, assuming that the free volume increases linearly with temperature it can be shown, for example, Ref. 10, that the Doolittle equation is equivalent to the Vogel-Fulcher-Tamman-Hesse (VFTH) equation (11-13), which can be formulated via the quantity θ in a few possible forms, for example:

$$\theta = \frac{E}{R(T - T_c)} \tag{7}$$

where R is gas constant, T is temperature, E is flow activation energy, T_c is the material constant.

For $T_c = 0$ the Arrhenius equation is obtained. *Equations 5* and *6* can be also used to account for the effect of pressure (decreasing the free volume) on viscosity, for example, Ref. 10.

Similarly, it can be assumed in this case that the existence of flow increases the mobility of molecules. As a consequence the free volume changes in respect to the state without flow appear. Such assumption was used by La Mantia [14, 15], who proposed a constitutive equation of the Maxwell type with discrete spectrum of relaxation times, which depend on the free volume according to the Doolittle formula. He assumed also, that the free volume changes (with respect to the state without flow) are proportional to the amount of elastic energy stored in the flowing liquid, that is, approximately to the first invariant of the stress tensor. Such formulation is not always possible, for example, for non-Newtonian (viscous or viscoplastic) systems, in which the elasticity is negligibly small or plays a secondary role. However, it can be generally assumed that the free volume in flow deviates (positively or negatively) from its equilibrium value in the state without flow. The present analysis relies on the assumption that the rate of absolute deviations is the difference between the rate of their creation and the rate of their decay. The rate of creation depends on the stress intensity $\tau = \sqrt{0.5 II_T}$ expressed by the second invariant of the extra-stress tensor. Simultaneously, the rate of decay is determined by the deviation magnitude from the state without flow. Within a semi-empirical approach confirmed by experimental data discussed later it was further assumed that the rate of creation can be expressed with a power-law function of the stress. In such case the following kinetic equation for the absolute relative free volume changes can be formulated:

$$\frac{d}{dt}\left|\frac{V_{fr}}{V_{fro}} - 1\right| = \frac{a}{\lambda_0}\tau^n - \frac{1}{\lambda}\left|\frac{V_{fr}}{V_{fro}} - 1\right| \tag{8}$$

where V_{fr}, V_{fro} are the free volume in flow and without flow, respectively, λ is the free volume relaxation time, a, n, λ_o are the material constants (the ratio a/λ_o is used only for convenience).

It can also be assumed that according to observations [1, 16] the stress action makes the relaxation times of various processes shorter. Therefore, for the parameter λ in *Eq. 8* as a function of stress the following simple expression was used:

$$\lambda = \frac{\lambda_0}{1 + b\tau^n} \tag{9}$$

where $b > a$ is a new material constant. The assumption $b > a$ means that the positive or negative free volume deviations from the rest state relax with increasing shear stress more quickly than they are created, that is, at enough high stresses the rates of creation and relaxation become equal.

In the steady flow the time derivative in *Eq. 8* is equal to zero. Hence, with the use of the *Eq. 9* the following formula for the free volume in flow V_{fr} in respect to the free volume without flow V_{fr0} results:

$$\left|\frac{V_{fr}}{V_{fro}} - 1\right| = \frac{a\tau^n}{1 + b\tau^n} \tag{10}$$

The Doolittle equation (*Eq. 5*) can be formulated both for enough large stresses (characterized by η, V_{fr}, θ) and for very small stresses (i.e. Newtonian flow region characterized by η_0, V_{fr0}, θ_0).

Eliminating the constant K from both expressions and using the *Eq. 10* one obtains two following viscosity models:

a. Positive deviations ($V_{fr} > V_{fro}$)—pseudoplastic behavior

$$\eta = \eta_0 \exp\left(-\theta_0 \frac{a\tau^n}{1 + (b + a)\tau^n}\right) \tag{11}$$

b. Negative deviations ($V_{fr} < V_{fro}$)—dilatant behavior

$$\eta = \eta_0 \exp\left(\theta_0 \frac{a\tau^n}{1 + (b - a)\tau^n}\right) \tag{12}$$

It should be noted that the parameter θ_0 can be (if necessary) determined independently from the VFTH equation or the Arrhenius equation if $T_c = 0$:

$$\theta_0 = \frac{E_0}{R(T - T_c)} \tag{13}$$

where E_0 is the flow activation energy in the Newtonian region.

DOI 10.1002/pen

Equations 11 and *12* along with the Doolittle *Eq. 5* make possible to calculate the flow activation energy at a constant stress. For the pseudoplastic behavior taken as example the following result is obtained:

$$E_\tau = E_0 \frac{1+b\tau^n}{1+(b+a)\tau^n} \tag{14}$$

Because the parameters a and b are usually small and in addition $b > a$, the value of E_τ changes slightly with the change of stress (in contrast to the flow activation energy at a constant shear rate). For this reason in typical flow conditions E_τ is almost the same as the flow activation energy E_0 in the (lower) Newtonian region. It was confirmed many times, for example, Ref. 17.

It should be also noted, that *Eqs. 11* and *12* predict the existence of the upper Newtonian viscosity η_∞ both for pseudoplastic and dilatant behavior, but it does not appear as the separate model parameter contrary to many other equations discussed later.

For practical purpose it is more convenient to represent the *Eqs. 11* and *12* in the following common form of the four-parameter model, which will be used hereafter:

$$\eta = \eta_0 \exp\left(-\frac{\delta\tau^n}{1+\alpha\tau^n}\right) \tag{15}$$

It can easily be verified that for $\delta < 0$, $\delta = 0$, and $\delta > 0$ one obtains the dilatant, Newtonian, and pseudoplastic behavior with ($\alpha > 0$) or without ($\alpha = 0$) the upper viscosity limit.

For $\alpha > 0$ the *Eq. 15* is a model with $\eta_\infty > 0$. Because typical flows proceed at moderate shear stresses, the *Eq. 15* can be simplified by neglecting the small term $\alpha\tau^n$ in the fraction's denominator. It leads to the approximate three-parameter model with $\eta_\infty = 0$ in the form of the Kohlrausch function [43]:

$$\eta = \eta_0 \exp(-\delta\tau^n) \tag{16}$$

By expanding the exponential *Eq. 16* with $\delta > 0$ into power series restricted to the first two terms, the well-known (till now purely empirical) Ellis model [3, 8] can be obtained:

$$\frac{\eta}{\eta_0} = \exp(-\delta\tau^n) = \frac{1}{\exp(\delta\tau^n)} \approx \frac{1}{1+\delta\tau^n} \tag{17}$$

It is noteworthy that similar power series expansion of the *Eq. 15* with $\delta > 0$ leads also to the model of Ellis type but with the non-zero upper Newtonian viscosity η_∞ as the new parameter. It is known sometimes as the Meter equation (19) and has the form:

$$\frac{\eta-\eta_\infty}{\eta_0-\eta_\infty} = \frac{1}{1+\varphi\tau^n} \tag{18}$$

where in this case $\eta_\infty = \eta_o\alpha/(\delta+\alpha)$ and $\varphi = (\delta+\alpha)$.

The proposed *Eq. 15* is probably the first stress dependent viscosity model, which is able to reflect quantitatively all possible types of viscous behavior that will be shown below.

For description of the flow curves in systems which have a complex rheological behavior, that is, different flow behavior in different shear stress or shear rate ranges, the so-called multimode models can be applied. Such models should be treated as products of two or more single modes. For the *Eq. 15* as the single mode the multimode equation has the form:

$$\eta = \eta_0 \exp\left(-\sum_i \frac{\delta_i \tau^{n_i}}{1+\alpha_i \tau^{n_i}}\right) \tag{19}$$

Till now, only some shear-rate dependent multimode models were applied for quantitative description of viscosity curves in systems with complex rheological behavior [18, 20, 21]. The applications of other models of this type as well as of the multimode stress dependent *Eq. 19* that retains the structure of the single mode will be discussed later.

It should be additionally noted that the number of modes in any multimode equation (stress or strain-rate dependent) is most frequently equal to the number of regions with dilatant or pseudoplastic behavior separated by regions of (approximately) Newtonian behavior.

It should be also noted that all models representing the viscosity as a function of the shear stress have their inverse forms representing the viscosity as corresponding functions of the shear rate. The inverse equation has a parametric form, which can easily be formulated using the equation of the flow curve. If the original viscosity equation has the form $\eta = f(\tau)$, than the inverse equation $\eta = g(\dot\gamma)$ has the following parametric representation:

$$\eta = f(\tau) \tag{20}$$

$$\dot\gamma = \frac{\tau}{f(\tau)} \tag{21}$$

with the shear stress τ as the parameter.

The same statement applies also for the shear-rate dependent models, that is, if the original viscosity equation is represented by $\eta = g(\dot\gamma)$, than the parametric form of the inverse equation $\eta = f(\tau)$ can be formulated as:

$$\eta = g(\dot\gamma) \tag{22}$$

$$\tau = g(\dot\gamma) \cdot \dot\gamma \tag{23}$$

where the parameter is the shear rate $\dot\gamma$.

EXPERIMENTAL VALIDATION OF STRESS DEPENDENT MODELS

It was already mentioned that within experimental appraisal of the proposed models the main attention will be focused on the *Eq. 15* or its simplified version (for $\alpha = 0$) in the form of the Kohlrausch function (*Eq. 16*) as well as on the multimode model (*Eq. 19*).

Figure 1 shows the comparison of predictions of the Kohlrauch type model with experimental data for the IUPAC-LDPE melt at 150°C [22] and 11.5% solution of polyisobutylene (PIB) in tetramethylpentadecane (TMPD) at 0°C [23].

It can be seen from Fig. 1 that the Kohlrausch equation *16* describes the experimental data in both cases very well within the range of shear stress and viscosity changes of many orders of magnitude. The model curves in Fig. 1 correspond to the following parameters in the *Eq. 16*: $\eta_0 = 55{,}000$ Pa s, $n = 0.479$, $\delta = 1.565 \cdot \times\ 10^{-2}$ Pa^{-n} for LDPE melt and $\eta_0 = 387.8$ Pa s, $n = 1.089$, $\delta = 2.085 \cdot \times\ 10^{-3}$ Pa^{-n} for PIB solution. A very good

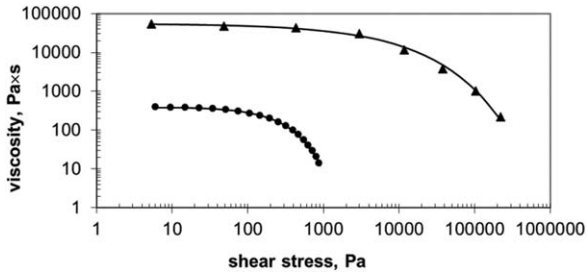

FIG. 1. Viscosity curves measured for LDPE melt (triangles) and PIB solution (circles) and predicted by the Kohlrausch equation (solid lines).

data description is possible because the experimental viscosity curves represented in double-logarithmic coordinates have an apparent curvature (variable slope) within the whole shear stress measurement range, that is, no power-law region appears. Such behavior is frequently observed for many polymer melts and solutions. Hence, the simple three-parameter shear-stress dependent model (*Eq. 16*), which predicts no power law behavior, is as a rule a very good model for quantitative description of their viscosity curves. The Ellis model (*Eq. 17*) which predicts the power-law region is in such cases inadequate. It is obvious that the more general four-parameter model (*Eq. 15*) describes the experimental data from Fig. 1 equally well. It will be shown later that the model (*Eq. 15*) is also able to represent the viscosity curves with power-law behavior.

Figure 2 shows as examples the predictions of the inverse model compared with experimental measurements for the same LDPE melt and PIB solution as in the Fig. 1. The parametric forms of corresponding inverse models for both liquids were calculated from *Eqs. 20* and *21* assuming the constants from the Fig. 1. It can be seen that the data fit is also very good as in the case of the stress dependent Kohlrausch equation. Additionally, it is noteworthy that both inverse equations predict almost constant slope of the viscosity curve in double-logarithmic coordinates, that is, the power-law region, for higher shear rates, while the corresponding stress dependent Kohlrausch functions have variable slopes in the whole shear stress range. For this reason a shear-rate dependent Kohlrausch function structurally the same as in the *Eq. 16* is not a good model for the description of viscosity curves. It is also shown as example in the Fig. 2 for the LDPE melt. The data fit is bad especially for high shear rates (the best fit was obtained for: $\eta_0 = 55{,}000$ Pa s, $n = 0.317$, $\delta = 1.005$ s^{-n}). It is a typical behavior of such model contrary to the shear-stress dependent analogue.

Figure 3 shows two examples of more complex pseudoplastic behavior, which requires the use of the full model (*Eq. 15*) to obtain the adequate description of the viscosity curve. The first one is the curve with the inflexion point, which is a characteristic feature for the existence of the upper viscosity limit η_∞. A typical example with apparent value of η_∞ is demonstrated for the blend of novolac (Nov) with 30% of natural rubber (30NR) at 140°C. The data come from own investigations. Some experimental results on various (not only rheological) properties of blends of novolack resins with epoxidized or non-epoxidized elastomers were reported in the work [24]. It is evident that the four-parameter model (*Eq. 15*) provides for $\eta_0 = 17{,}900$ Pa s, $n = 1.832$, $\delta = 1.58 \cdot \times\ 10^{-6}$ Pa^{-n}, $\alpha = 3.25 \cdot \times\ 10^{-7}$ Pa^{-n} an excellent fit of the theoretical curve to experimental data. A good fit is also possible using the four-parameter Meter model (*Eq. 18*) for $\eta_0 = 17{,}900$ Pa s, $\eta_\infty = 140$ Pa s, $n = 2.445$, $\varphi = 3.09 \cdot \times\ 10^{-8}$ Pa^{-n}.

It was mentioned earlier that the Kohlrausch function (*Eq. 16*) is not able to describe adequately the stress dependent viscosity curves with power law region. As an example, where the full model (*Eq. 15*) must be used although no upper viscosity limit appears, the viscosity curve for the blend of novolac resin and 10% epoxidized natural rubber with 25% epoxidation degree (10ENR25) at 140°C is also shown in the Fig. 3. It is easily seen that the experimental curve has an almost constant slope, that is, the power-law region, for the last few points. It is evident from Fig. 3 that the Kohlrausch function (*Eq. 16*) with the best fit for $\eta_0 = 4{,}810$ Pa s, $n = 1.538$, $\delta = 6.44 \cdot \times\ 10^{-7}$ Pa^{-n} underestimates the true values for high stresses, while the full model (*Eq. 15*) with $\eta_0 = 4{,}810$ Pa s, $n = 1.432$, $\delta = 1.45 \cdot \times\ 10^{-6}$ Pa^{-n}, $\alpha = 2.46 \cdot \times\ 10^{-7}$ Pa^{-n} provides a very good fit. In such case the more simple three-parameter Ellis *Eq. 17* provides also a quite good fit to experimental data for $\eta_0 = 4{,}870$ Pa s, $n = 1.927$, $\delta = 4.02 \cdot \times\ 10^{-8}$ Pa^{-n}.

The simple four-constant model (*Eq. 15*) is also able to describe very well the viscosity curves of the very shear-thinning liquids, that is, liquids with a huge viscosity jump within a very narrow shear stress interval. Such systems were discussed by Roberts et al. [25], who used for their description "composite Ellis model," that is, the Ellis (Meter) model (*Eq. 18*) with parameters η_o and η_∞, which are also Ellis-type

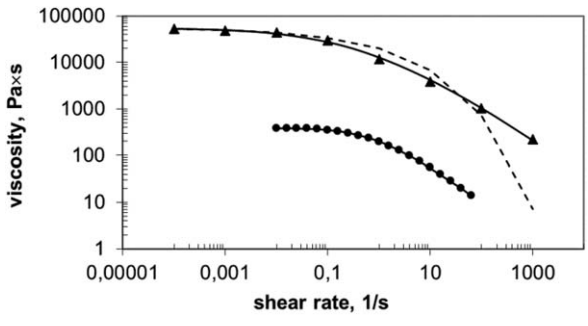

FIG. 2. Viscosity curves predicted by inverse viscosity equations (solid lines) compared with experimental data for LDPE melt (triangles) and PIB solution (circles) and with the shear-rate dependent Kohlrausch function for LDPE (dotted line).

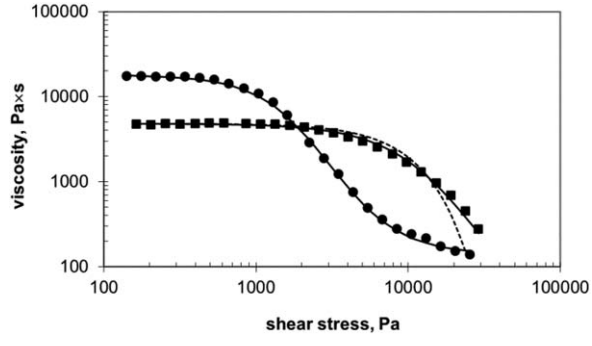

FIG. 3. Experimental viscosity curves for Nov-30NR blend (circles) and Nov-10ENR25 blend (squares) compared with predictions of model (*Eq. 15*) (solid lines) for both blends and Kohlrausch function (dotted line) for Nov-10ENR25.

DOI 10.1002/pen

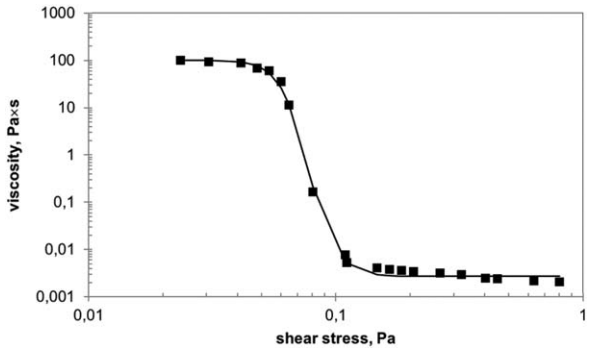

FIG. 4. Comparison of experimental viscosity curves for a saliva (squares) and calculated (solid line) from equation (*Eq. 15*).

functions of the shear stress. Figure 4 shows as an example the comparison of the experimental viscosity curve for a saliva (taken from the Roberts' article) with prediction of the *Eq. 15*, which is simpler and includes less number of parameters then the original eight-constant "composite Ellis model." It can be seen that the fit of theoretical curve resulting from model (*Eq. 15*) for $\eta_0 = 101.45$ Pa s, $n = 7.595$, $\delta = 2.927 \cdot \times\ 10^9$ Pa^{-n}, $\alpha = 2.781 \cdot \times\ 10^8$ Pa^{-n} to experimental data is very good taking into account the small number of parameters (four instead of eight). The parameter values are in this case very large in comparison with similar values for other systems discussed earlier.

Such a large viscosity jump (ca. 4 orders of magnitude within the shear stress interval of 0.05 Pa in this case) is typical of viscoplastic behavior characterized by a yield stress τ_y. Assuming that the yield stress value corresponds to the maximal slope $d\ln\eta/d\ln\tau$, that is, the inflection point, of the viscosity curve it can be shown with the use of the *Eq. 15* that

$$\tau_y = \alpha^{-\frac{1}{n}} \tag{24}$$

For the data in Fig. 4 $\tau_y = 0.077$ Pa.

The next examples shown in Fig. 5 deal with the description of a pure dilatant behavior with the discussed stress-dependent models. Such behavior was found for suspension of 57 vol% polystyrene (PS) in glycerol/water mixture at 20°C [26] and in own viscosity measurements of novolac (Nov)—epoxidized natural rubber (ENR) blends for Nov-10ENR50 (10 wt% of ENR with epoxidation degree 50%) at 140°C. The viscosity rise without the upper limit was observed in this case for low shear rates (below a few s^{-1}) but high shear stresses. It is probably due to the creation of considerable long chain branching by interchain reactions during blending, although the blends were stable in time during the viscosity measurement. Another Nov-ENR blends were presented earlier. It is interesting to note that blends of novolacs with epoxidized and nonepoxidized elastomers have a very different, sometimes unexpected, rheological behavior. For instance, the replacement of ENR25 by the same amount of ENR50 changes completely the blend behavior from pure pseudoplastic (Fig. 3) to pure dilatant (Fig. 5). It follows from Fig. 5 that the shear-stress dependent viscosity curve for dilatant behavior of Nov-10ENR50 blend can also be adequately described by the Kohlrausch function with the parameters $\eta_0 = 9{,}230$ Pa s, $n = 1.383$, $\delta = -1.18 \cdot \times\ 10^{-6}$ Pa^{-n}. The second dilatant system—PS suspension—shown in Fig. 5 possesses the upper Newtonian viscosity. Therefore, for its description the full model (*Eq. 15*) must be applied. It is evident that this model with $\eta_0 = 847$ Pa s, $n = 0.9533$, $\delta = -0.01933$ Pa^{-n}, $\alpha = 0.0586$ Pa^{-n} fits very well to experimental data that confirms its practical utility in description of various viscosity curves.

The quantitative description of more complicated viscosity curves requires the application of the multimode model (*Eq. 19*), most frequently of the two-mode model. Three examples of the viscosity curves, which can be described by the two-mode equations are given below.

The first one shown in Fig. 6 concerns also a class of very shear-thinning liquids somewhat similar to those discussed above but without the upper viscosity limit. It is characteristic of pseudoplastic melts of branched polymers, polymers with a broad MWD, or some polymer blends. The viscosity curve as a function of shear rate have in double logarithmic coordinates a very broad transition zone between Newtonian and power law behavior. This results sometimes in very sharp viscosity changes, especially at high shear stresses or shear rates (the power law exponent is close to 0). Such changes cannot be quantitatively well described by typical viscosity models. A two-mode shear-rate dependent model based on the Carreau-Yasuda equation was used by Stadler and Münstedt [21] for this purpose. In this case, the simple Kohlrausch function (*Eq. 16*) is not able to describe quantitatively the curve in the Fig. 6. However, it is possible when using the two-mode five-parameter model in the form of the product of two Kohlrausch functions:

$$\eta = \eta_0 \exp(-\delta_1 \tau^{n_1} - \delta_2 \tau^{n_2}) \tag{25}$$

It can be seen that the parameters $\eta_0 = 10{,}500$ Pa s, $n_1 = 1.12$, $\delta_1 = 3 \cdot \times\ 10^{-5}$ Pa^{-n}, $n_2 = 7.89$, $\delta_2 = 8 \cdot \times\ 10^{-35}$ Pa^{-n}

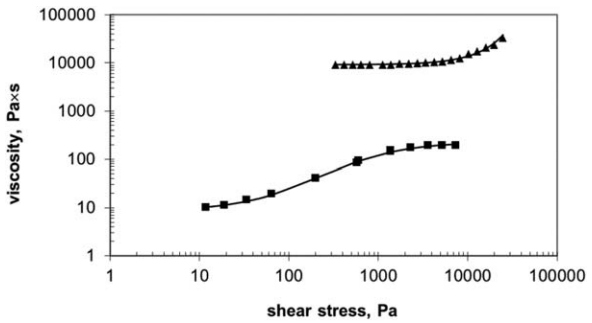

FIG. 5. Comparison of measured viscosity curve for Nov-10ENR50 blend (triangles) and PS suspension (squares) with predictions (solid lines) of model (*Eqs. 16* and *15*), respectively.

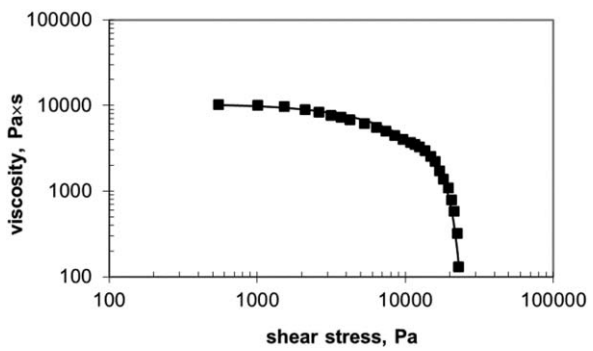

FIG. 6. Comparison of viscosity curves for PE-LD/PP (1:1) blend measured (squares) and calculated (solid line) from equation (*Eq. 25*).

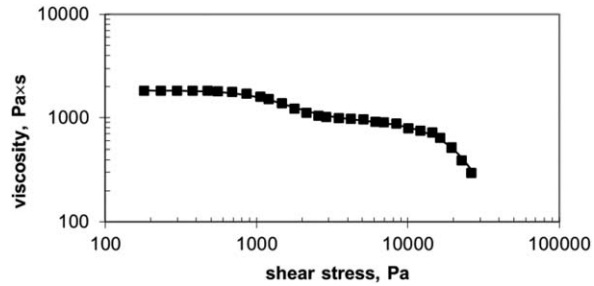

FIG. 7. Comparison of viscosity curves measured (squares) and calculated (solid line) from equation (*Eq. 26*) for PA12-10%SBS blend.

of both modes in *Eq. 25* used for description of the viscosity curve of LDPE/PP (1:1) blend at 190°C taken as example from own measurements are extremely different.

The second example presented in Fig. 7 is typical of systems, which change their phase structure during flow, such as liquid-crystalline polymers, block thermoplastic elastomers and different blends. Such behavior was also observed in some blends of novolac with elastomers mentioned above and the blends of aliphatic polyamides with epoxidized and nonepoxidized elastomers [27]. In Fig. 7, the blend of PA12 with 10% of SBS block copolymer at 200°C is shown. The flow curve consists of two regions with pseudoplastic behavior—the first one with and the second one without the upper viscosity limit. Hence, the corresponding two-mode six-parameter viscosity equation has the following form:

$$\eta=\eta_0\exp\left(-\frac{\delta_1\tau^{n_1}}{1+\alpha_1\tau^{n_1}}-\delta_2\tau^{n_2}\right) \tag{26}$$

A very good fit of the model curve obtained for $\eta_0 = 1{,}840$ Pa s, $n_1 = 2.716$, $\delta_1 = 1.29\cdot\times\ 10^{-9}$ Pa^{-n}, $\alpha_1 = 1.98\cdot\times\ 10^{-9}$ Pa^{-n}, $n_2 = 1.981$, $\delta_2 = 3.40\cdot\times\ 10^{-9}$ Pa^{-n} confirms the practical utility of the two-mode model (*Eq. 26*) for description of the curves with the characteristic course shown in the Fig. 7.

The third example shown in Fig. 8 concerns the viscosity curves consisting of two regions with pseudoplastic and dilatant behavior both with lower and upper viscosity limits. Hence, the corresponding two-mode equation should have the form of the seven-parameter model:

$$\eta=\eta_0\exp\left(-\frac{\delta_1\tau^{n_1}}{1+\alpha_1\tau^{n_1}}-\frac{\delta_2\tau^{n_2}}{1+\alpha_2\tau^{n_2}}\right) \tag{27}$$

In this case the experimental data for 55% cornstarch suspension in water at 25°C were taken from Ref. 28. It can be seen

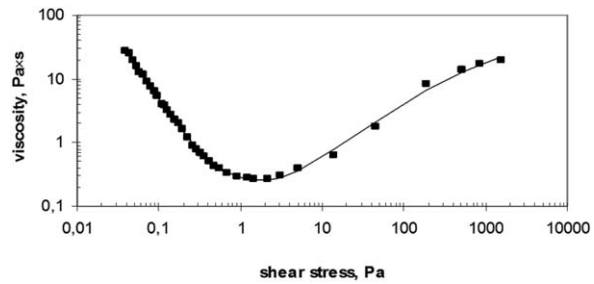

FIG. 8. Comparison of viscosity curves measured (squares) and calculated (solid line) from equation (*Eq. 27*) for water cornstarch suspension.

that the agreement of experimental data and theoretical predictions based on *Eq. 27* with $\eta_0 = 66.4$ Pa s, $n_1 = 0.563$, $\delta_1 = 125$ Pa^{-n}, $\alpha_1 = 3.59$ Pa^{-n}, $n_2 = 0.358$, $\delta_2 = -57.2$ Pa^{-n}, $\alpha_2 = 1.64$ Pa^{-n} is also very good taking into account the complicated course of the measured viscosity curve. It testifies to the flexibility of the multimode stress dependent model in description of more complex rheological behavior of non-Newtonian liquids.

STRAIN-RATE DEPENDENT VISCOSITY MODELS

Another, much more popular group of viscosity equations is created by making the viscosity dependent on the rate-of-strain, most frequently on the shear rate. Several well-known models, such as those of Carreau [29], Carreau-Yasuda et al. [30], and Cross [31] belong to this group. Here, the two shear-rate dependent models are assessed.

The first one is an analogue of the shear-stress dependent *Eq. 15*:

$$\eta=\eta_o\exp\left(-\frac{\varepsilon\dot{\gamma}^m}{1+\beta\dot{\gamma}^m}\right) \tag{28}$$

where η_o, β, ε, and m are material constants.

Equation 28 can be derived in the same way as the model (*Eq. 15*) by assuming that the free volume changes during flow depend on the shear rate instead of shear stress. It should be also mentioned that the equivalents of the Ellis and Meter equations (*17* and *18*) are in this case the Cross equations without and with the upper viscosity limit. The flow activation energy at a constant shear rate $E_{\dot{\gamma}}$ can be also similarly defined as the flow activation energy at a constant shear stress E_τ in the *Eq. 14*.

The model (*Eq. 28*) was tested using the experimental data for the same liquids, which were applied for assessment of the shear-stress dependent model (*Eq. 15*). It should be generally stated that the *Eq. 28* provides a good description of viscosity curves without upper viscosity limit. For instance, the model viscosity curves for LDPE melt and PIB solution resulting from *Eq. 28* with the parameters: $\eta_0 = 61{,}190$ Pa s, $m = 0.325$, $\varepsilon = 1.941$ s^{-m}, $\beta = 0.241$ s^{-m} (LDPE at 150°C) and $\eta_0 = 437.4$ Pa s, $m = 0.533$, $\varepsilon = 0.918$ s^{-m}, $\beta = 0.154$ s^{-m} (PIB solution in TMPD at 0°C) overlap practically the corresponding curves shown in Fig. 2 for the inverse stress dependent Kolhlrausch model. However, the *Eq. 28* requires four constants, while the Kohlrausch function (*Eq. 16*) is the three-parameter model and its shear-rate dependent equivalent is obviously inadequate that was also demonstrated in Fig. 2. For more complicated viscosity curves, that is, curves with upper viscosity limit or those which require the use of multimode equation, the description accuracy of the model (*Eq. 28*) is apparently lower in comparison with the stress dependent model (*Eq. 15*) or the new shear-rate dependent equation presented below. Such behavior is probably due to the fact that the assumption the free volume changes during flow depend on the shear rate intensity (instead of the shear stress intensity) is not fulfilled.

The second shear-rate dependent viscosity equation originates from material functions predicted by some phenomenological constitutive equations, such as the eight-constant Oldroyd model [8]. Various specific cases of this model (containing different numbers of constants) predict for the simple shear flow the viscosity function, which can be generally formulated as:

DOI 10.1002/pen

$$\eta=\eta_o\frac{1+(\lambda_1\dot{\gamma})^2}{1+(\lambda_2\dot{\gamma})^2} \tag{29}$$

where η_0, λ_1, λ_2 are the non-negative material constants, $\dot{\gamma}$ is the shear rate.

By introducing two further non-negative constants μ and v, *Eq. 29* can be generalized to the form of a flexible five-constant model:

$$\eta=\eta_o\left[\frac{1+(\lambda_1\dot{\gamma})^v}{1+(\lambda_2\dot{\gamma})^v}\right]^\mu \tag{30}$$

The following cases determined by the values of constants λ_i result from the expression (*Eq. 30*):

1. Newtonian liquid: $\lambda_1=\lambda_2=0$
2. Pseudoplastic liquid with upper viscosity limit: $0<\lambda_1<\lambda_2$
3. Pseudoplastic liquid without upper viscosity limit (viscosity decreases to 0): $\lambda_2>\lambda_1=0$
4. Dilatant liquid with upper viscosity limit: $\lambda_1>\lambda_2>0$
5. Dilatant liquid without upper viscosity limit (viscosity increases to infinity): $\lambda_1>\lambda_2=0$

In the general case the shear rate $\dot{\gamma}$ in *Eqs. 28* and *30* should be replaced by the function of the second invariant of the rate-of-strain tensor D, that is, $\dot{\gamma}=\sqrt{0.5II_D}$.

For more detailed choice of constants, *Eq. 30* contains a variety of less or more known three- or four-parameter models, such as for example ($\lambda_1=0$):

a. Four-parameter Carreau-Yasuda et al. equation (30)

$$\eta=\frac{\eta_o}{[1+(\lambda_2\dot{\gamma})^v]^\mu} \tag{31}$$

b. Three-parameter Carreau equation, that is, Carreau-Yasuda equation for $v=2$ [29]
c. Three-parameter Cross equation, that is, Carreau-Yasuda equation for $\mu=1$ [31].

Equations a–c describe only the pseudoplastic behavior without upper viscosity limit, but their dilatant counterparts can be easily obtained taking $\lambda_1\neq0$ and $\lambda_2=0$ in expression (*Eq. 30*).

Another general method to formulate equations with non-zero upper viscosity limit is the pseudo-linear combination of the upper Newtonian viscosity value η_∞ with a suitable equation for pseudoplastic behavior without upper viscosity limit. It will be shown using as example the Carreau-Yasuda model (*Eq. 31*), that corresponds to the lack of non-zero upper viscosity limit.

$$\eta=\frac{\eta_o-\eta_\infty}{[1+(\lambda_2\dot{\gamma})^v]^\mu}+\eta_\infty \tag{32}$$

After a simple transformation one obtains the typical form:

$$\frac{\eta-\eta_\infty}{\eta_o-\eta_\infty}=\frac{1}{[1+(\lambda_2\dot{\gamma})^v]^\mu} \tag{33}$$

where $\eta_o>\eta_\infty$ stands for the pseudoplastic behavior and $\eta_o<\eta_\infty$ for the dilatant one.

Equation 33 has the same number of adjustable constants as the model (*Eq. 30*) in which the upper viscosity limit η_∞ does not appear as a separate parameter. Quite similar relationship as described by expression (*Eq. 33*) exists also formally between the stress dependent Ellis and Meter *Eqs. 17* and *18*.

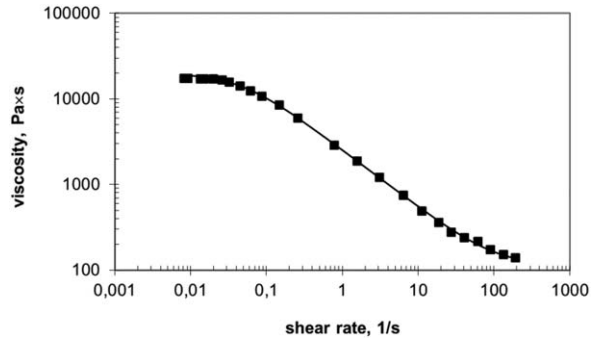

FIG. 9. Comparison of experimental viscosity curve (squares) for Nov-30NR blend with predictions of the model (*Eq. 30*) (solid line).

It is interesting to compare the behavior of the shear-stress dependent model (*Eq. 15*) with the shear-rate dependent model (*Eq. 30*) using the same set of data for the Nov-30NR blend. The corresponding plots for the models (*Eqs. 15* and *30*) are shown in Figs. 3 and 9, respectively. It can be seen from Fig. 9, that the *Eq. 30* with $\eta_0=17{,}968$ Pa s, $\lambda_1=9.7\cdot\times\ 10^{-3}$ s, $\lambda_2=21.7$ s, $\mu=0.5037$, $v=1.3297$ provides also a very good fit to the experimental curve confirming its utility for description of viscosity curves. It can be shown that the viscosity curve resulting from any of the two equations practically overlaps the curve obtained from the second inverted equation. However, the shear-rate dependent equation *30* is the five-parameter model, while the shear-stress dependent model (*Eq. 15*) requires only four constants, that is, it seems to be more efficient in description of the viscosity curves.

For the description of more complicated viscosity curves by means of shear-rate dependent equations the multimode models can also be applied. The multimode model generated by the equation *30* has the structure:

$$\eta=\eta_o\prod_i\left[\frac{1+(\lambda_{1i}\dot{\gamma})^{v_i}}{1+(\lambda_{2i}\dot{\gamma})^{v_i}}\right]^{\mu_i} \tag{34}$$

It is noteworthy that some viscosity equations known from literature can be formally treated as two-mode equations with modes defined by other models. For instance, the four-parameter Vinogradov–Malkin equation (32):

$$\eta=\frac{\eta_o}{1+(\lambda_1\dot{\gamma})^v+(\lambda_2\dot{\gamma})^{2v}} \tag{35}$$

is formally a product of two modes resulting from the Cross equation with the same values of the exponent v and different values of the time constants λ.

Another useful example is the four-parameter extended Carreau equation *20*:

$$\eta=\frac{\eta_o}{\left[1+\kappa(\lambda\dot{\gamma})^2+(\lambda\dot{\gamma})^4\right]^{\frac{\mu}{4}}} \tag{36}$$

Equation 36 was initially introduced by replacing the shear-rate dependent binomial in the Carreau equation by polynomial with even powers of shear rate (in this case the polynomial of 4th order)

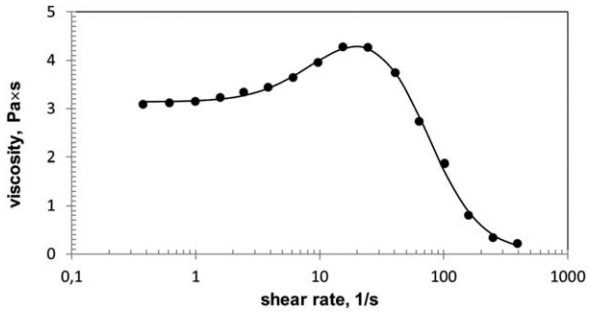

FIG. 10. Viscosity curve of aqueous solution of urethane-coupled PEO at 25°C experimental data (full circles), equation (*Eq. 37*) (solid line).

[20]. On the other hand, *Eq. 36* can be treated as the product of two modes resulting from Carreau equation with the same values of exponent μ and different values of time constants or as the geometric mean (square root) from product of two Carreau equations with the above properties. For $\kappa = 2$, *Eq. 36* becomes the Carreau equation, and for $\kappa > 2$ its properties are similar to the Carreau-Yasuda model, that is, both equations describe very well the viscosity curves with a wide transition range between Newtonian and power law behavior [20, 33]. For $\kappa < 2$ it is also able to describe more rapid changes between both regions.

The models (*Eqs. 35* and *36*) can be also easily transformed to forms with the upper viscosity limit according to *Eqs. 32* and *33* applied for the Carreau-Yasuda model.

It was found that in many cases the two-mode models of the type (*Eq. 34*) with even v_i-values (most frequently $v_i = 2$ or 4) are able to represent quantitatively very complex behavior [20]. It will be also demonstrated here using numerical data on viscosity measurements for the aqueous solution of urethane-coupled poly(ethylene oxide) at 25°C quoted by Lashkarbolok et al. [34], which are presented in the Fig. 10.

It can be seen that the experimental viscosity curve has two regions with dilatant and pseudoplastic behavior, both with lower and upper viscosity limits. Therefore, as the appropriate viscosity equation the following two-mode seven-parameter model (with preselected $v_1 = v_2 = 2$) was chosen:

$$\eta = \eta_0 \left[\frac{1+(\lambda_1\dot{\gamma})^{v_1}}{1+(\lambda_2\dot{\gamma})^{v_1}}\right]^{\mu_1} \left[\frac{1+(\lambda_3\dot{\gamma})^{v_2}}{1+(\lambda_4\dot{\gamma})^{v_2}}\right]^{\mu_2} \tag{37}$$

It follows from Fig. 10 that the *Eq. 37* with $\eta_o = 3.140$ Pa s, $\lambda_1 = 0.2274$ s, $\lambda_2 = 0.0569$ s, $\lambda_3 = 0$ s, $\lambda_4 = 0.0138$ s, $\mu_1 = 0.1708$, $\mu_2 = 0.9942$ describes perfectly the experimental data.

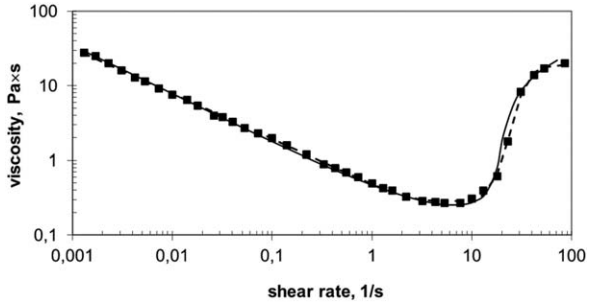

FIG. 11. Comparison of experimental data (squares) for water cornstarch suspension with predictions of the inverse viscosity model (*Eq. 27*) (solid line) and the model (*Eq. 37*) (dotted line).

In some cases a better description of experimental data can be obtained assuming that the v_i values are not preselected. However, in such case the number of model constants increases.

Figure 11 presents the comparison of experimental data for the cornstarch suspension discussed earlier (Fig. 8) with the regression curve resulting from the *Eq. 37* for $\eta_o = 56.55$ Pa s, $\lambda_1 = 0.4151$ s, $\lambda_2 = 2{,}600.2$ s, $\lambda_3 = 0.0452$ s, $\lambda_4 = 0.0384$ s, $\mu_1 = 0.1771$, $\mu_2 = 5.2817$, $v_1 = 3.4249$, $v_2 = 4.9266$. To compare the quality of the shear rate and shear-stress dependent models the theoretical curve obtained from the inverted two-mode *Eq. 27* is also given.

It can be seen from Fig. 11 that both curves describe excellently the experimental data and their course is almost identical. Only in the dilatant region small differences appear. It is also obvious that the inverse equation provides equally good description of the experimental results as the shear-stress dependent model in Fig. 8. The same behavior was observed for more simple viscosity curves presented in Figs. 1 and 2. It seems to be a general property of all inverse models, that is, an adequate initial model leads to the adequate inverse model.

It is noteworthy that for description of complicated viscosity curves multiparameter models of other types were also proposed [35–40]. One of possible ways to create such models is a linear combination of a few more simple viscosity equations, for example, Ref. 35. A specific example of such combination is the equation *32*. A method of piecewise description of viscosity curves by means of the Cross equation with upper viscosity limit, which was modified to prevent continuity and differentiability of the resulting multiparameter function, was also presented [36–38]. Somewhat similar modification in form of the composite Ellis model discussed earlier [25] should be also mentioned. Another type of multiparameter models created with the use of exponentials was presented in the works [39, 40]. It is interesting to note that for testing of various models the data for starch suspensions [28] were frequently applied as one of examples. It gives the opportunity to compare the efficiency of various models in description of complex viscosity curves. It can be concluded that the model based on the modified Cross equation requires nine parameters to reflect adequately the experimental data [36], while the model based on exponential functions is the 10-parameter model [40]. The shear-rate dependent two-mode model (*Eq. 37*) requires also nine parameters assuming that the v_i values are arbitrary and not preselected as even numbers. On the other hand, the two-mode stress dependent model (*Eq. 27*) seems to be more efficient in description of experimental data for the starch suspension, because it requires only seven constants. The predictions of this equation in initial and inverse form are shown in Figs. 8 and 11. A very similar conclusion results also from the data for LDPE melt and PIB solution shown in Fig. 2. The corresponding viscosity curves are equally well described by the inverse three-constant shear-stress dependent Kohlrausch model and by the four-constant shear-rate dependent equation *28*. A better efficiency of the stress dependent models results also from the comparison of Figs. 3 and 9 obtained for the same set of data with the use of shear stress and shear-rate dependent models (*Eqs. 15* and *30*), respectively. An adequate description of experimental data in both cases requires four constants for the model (*Eq. 15*) and five constants for the model (*Eq. 30*).

CONCLUSIONS

Some new possibilities of quantitative description of viscosity curves in the steady shear flow of non-Newtonian fluids

DOI 10.1002/pen

were discussed. The main attention was focused on the shear-stress dependent models resulting from the concept of relaxation changes of the free volume during the shear flow. The obtained new viscosity model (*Eq. 15*), which contains more simple formulas, such as Kohlrausch function or Ellis and Meter equations as specific cases, is principally valid for pseudoplastic behavior. However, the comparison of model predictions with experimental data for several systems shows that it describes very well both pseudoplastic and dilatant behavior. It can be also generalized to the multimode model, which is a product of two or more initial equations (modes). The applicability of such models for the viscosity description of different liquid systems was tested. It was found that the new shear-stress dependent equations are able to describe very complicated viscosity curves with a great accuracy.

A new shear-rate dependent viscosity model (*Eq. 30*) based on modified shear viscosity function of the Oldroyd constitutive equation and multimode models in form of products of two or more modes defined by the initial model were also discussed and compared with experimental data. The proposed new model (*Eq. 30*) comprises a number of known viscosity equations, for example, Carreau-Yasuda, Carreau and Cross equations, as specific cases. The stress dependent models seem to be more efficient in comparison with the strain-rate dependent models, because they require a smaller number of adjustable constants to describe adequately the same set of data. This statement is also true for the inverse models defined in parametric form, which have the same number of parameters as the initial equation. The proposed *Eqs. 15* and *19* are probably the first stress dependent GNF models, which are able to describe adequately very complicated viscosity curves including those characteristic of viscoplastic behavior. Similar description quality provides also the shear-rate dependent new model in the simple form (*Eq. 30*) and its multimode form (*Eq. 34*). It should be also mentioned that the shear-rate dependent viscosity models discussed above can be essentially adapted for description of viscoplastic behavior, that is, the existence of the yield stress τ_y, by introducing this parameter into the equation of the flow curve to obtain:

$$\tau = \tau_y + \eta \cdot \dot{\gamma} \quad \text{for } \tau > \tau_y \tag{38a}$$

$$\dot{\gamma} = 0 \quad \text{for } \tau \leq \tau_y \tag{38b}$$

where the viscosity η as a function of shear rate is defined by any of viscosity equations discussed earlier. Various equations of the type (*Eqs.* 38a and 38b) for spatial description of viscoplastic behavior in terms of the rate-of strain tensor were reviewed, for example, Ref. 41. Dorigato et al. [42] used the Eqs. 38a and 38b with the viscosity defined by the Kohlrauch function corresponding to $\beta = 0$ in expression (*Eq. 28*) to describe quantitatively the results of oscillatory measurements of filled polyethylene with yield stress (in this case the shear rate $\dot{\gamma}$ was replaced by the oscillation frequency ω). However, the proper choice of the viscosity function in the Eqs. 38a and 38b requires experimental verification in the general case.

ABBREVIATIONS

ENR	epoxidized natural rubber
GNF	generalized Newtonian fluid
MWD	molecular weight distribution
Nov	novolac resin
NR	natural rubber
PA12	polyamide 12
PEO	poly(ethylene oxide)
PE-LD	low-density polyethylene
PE-LD/PP	low-density polyethylene/polypropylene blend
PIB	polyisobutylene
PS	polystyrene
SBS	styrene-butadiene-styrene block copolymer
TMPD	tetramethylpentadecane
VFTH	Vogel-Fulcher-Tamman-Hesse equation

REFERENCES

1. G.W.M. Peters, J.F.M. Schoonen, F.P.T. Baaijens, and H.E.H. Meijer, *J. Non-Newton. Fluid Mech.*, **82**, 387 (1999).
2. F. Yilmaz and M.Y. Gundogdu, *Korea Aust. Rheol. J.*, **20**, 197 (2008).
3. P.J. Carreau, D.C.R. DeKee, and R.P. Chhabra, *Rheology of Polymeric Systems*, Hanser, New York (1997).
4. M.A. Rao, *Rheology of Fluid and Semisolid Foods*, Springer, New York (2007).
5. D. Laba, Ed., *Rheological Properties of Cosmetics and Toiletries*, Marcel Dekker, New York (1993).
6. P. Coussot, *Mudflow Rheology and Dynamics*, Bolkema Publications, Rotterdam (1997).
7. R.G. Larson, *Constitutive Equations for Polymer Melts and Solutions*, Butterworths, Boston (1988).
8. R.B. Bird, R.C. Armstrong, and O. Hassager, *Dynamics of Polymeric Liquids, Vol. 1, Fluid Mechanics*, Wiley, New York (1987).
9. A.K. Doolittle, *J. Appl. Phys.*, **22**, 1471 (1951).
10. J.D. Ferry, *Viscoelastic Properties of Polymers*, Wiley, New York (1980).
11. H. Vogel, *Phys. Z.*, **9**, 645 (1921).
12. G.S. Fulcher, *J. Am. Ceram. Soc.*, **8**, 339 (1925).
13. G. Tammann and W. Hesse, *Z. Anorg. Allg. Chem.*, **156**, 245 (1926).
14. F.P. La Mantia, *Rheol. Acta*, **16**, 302 (1977).
15. F.P. La Mantia and G. Titomanlio, *Rheol. Acta*, **18**, 469 (1979).
16. Y. Seo, *J. Appl. Polym. Sci.*, **88**, 510 (2003).
17. A.V. Shenoy, *Rheology of Filled Polymer Systems*, Kluwer, Dordrecht (1999).
18. K. Yasuda, *J. Textile Eng.*, **52**, 171 (2005).
19. D.M. Meter and R.B. Bird, *AIChE J.*, **10**, 878 (1964).
20. R. Steller, *Polimery*, **58**, 81 (2013) (in Polish).
21. F.J. Stadler, and H. Münstedt, *J. Non-Newton Fluid Mech.*, **151**, 129 (2008).
22. J. Meissner, *Pure Appl. Chem.*, **42**, 551 (1975).
23. C.R. Schultheisz, S.D. Leigh, *NIST Special Publication*, National Institute of Standards and Technology, Gaithersburg 260 (2002), http://www.nist.gov/srm/upload/SP260-143.PDF
24. R. Steller, D. Zuchowska, W. Meissner, and G. Kedziora, *Polimery*, **57**, 470 (2012) (in Polish).
25. G.P. Roberts, H.A. Barnes, and P. Carew, *Chem. Eng. Sci.*, **56**, 5617 (2001).

26. W.H. Boersma, J. Laven, and H.N. Stein, *AIChE J.*, **36**, 321 (1990).
27. E. Micewicz, PhD thesis, Reactive processing of polyamides - epoxidized elastomers blends. Wroclaw University of Technology (2001) (in Polish).
28. E.E. Bishoff-White, M. Chellamuthu, and J.P. Rothstein, *Rheol. Acta*, **49**, 119 (2010).
29. P.J. Carreau, *Trans. Soc. Rheol.*, **16**, 99 (1972).
30. K. Yasuda, R.C. Armstrong, and R.E. Cohen, *Rheol. Acta*, **20**, 163 (1981).
31. M.M. Cross, In *Polymer Systems: Deformation and Flow*, R.E. Wetton and R.W. Whorlow, Eds., Macmillan, London (1968).
32. G.V. Vinogradov, A.Ya. Malkin, *Rheology of Polymers*, Mir Publishers, Moscow (1980)
33. J.M. Dealy, R.G. Larson, *Structure and Rheology of Molten Polymers: From Structure to Flow*, Hanser, Munich (2006).
34. M. Lashkarbolok, S. Izadi, H. Alemi, and S. Drost, *Korea-Aust. Rheol. J.*, **27**, 105 (2015).
35. J. Stastna, L. Zanzotto, and O.J. Vacin, *J. Colloid Interface Sci.*, **259**, 200 (2003).
36. F.J. Galindo-Rosales, F.J. Rubio-Hernández, and A. Sevilla, *J. Non-Newton. Fluid Mech.*, **166**, 321 (2011).
37. F.J. Galindo-Rosales, F.J. Rubio-Hernández, A. Sevilla, and R.H. Ewoldt, *J. Non-Newton. Fluid Mech.*, **166**, 1421 (2011).
38. P.R. Souza-Mendes, and E.S. Dutra, *Appl. Rheol.*, **14**, 296 (2004).
39. J. David, and P. Filip, *Appl. Rheol.*, **14**, 82 (2004).
40. J. David, P. Filip, and A.A. Kharlamov, *Adv. Mater. Sci. Eng.*, **2013**, 658187 (2013). dx.doi.org/10.1155/2013/658187
41. E. Mitsoulis, *Rheology Reviews*, British Society of Rheology, 135 (2007), the article, see: http://www.bsr.org.uk/rheology_review.asp
42. A. Dorigato, A. Pegoretti, and A. Penati, *eXPRESS Polym. Lett.*, **4**, 115 (2010).
43. R.S. Anderssen, S.A. Husain, and R.J. Loy, *Anzjam J.*, **45**, C800 (2004).

 DOI 10.1002/pen